Materials Science-Poland, 37(3), 2019, pp. 373-380
http://www.materialsscience.pwr.wroc.pl/
DOI: 10.2478/msp-2019-0038

SHI irradiation induced modifications of plasmonic properties of Ag-TiO_2 thin film and study using FDTD simulation

HIMANSHU SHARMA*, R. SINGHAL

Department of Physics, Malaviya National Institute of Technology, Jaipur, India

Modifications in morphological and plasmonic properties of heavily doped Ag-TiO_2 nanocomposite thin films by ion irradiation have been observed. The Ag-TiO_2 nanocomposite thin films were synthesized by RF co-sputtering and irradiated by 90 MeV Ni ions with different fluences. The modifications in morphological, structural and plasmonic properties of the nanocomposite thin films caused by ion irradiation were studied by transmission electron microscopy (TEM), X-ray diffraction (XRD), and UV-Vis absorption spectroscopy. The thickness of the film and concentration of Ag were assessed by Rutheford backscattering (RBS) as ∼50 nm and 56 at.%, respectively. Interestingly, localized surface plasmon resonance (LSPR) appeared at 566 nm in the thin film irradiated at the fluence of 1×10^{13} ions/cm^2. This plasmonic behavior can be attributed to the increment in interparticle separation. Increased interparticle separation diminishes the plasmonic coupling between the nanoparticles and the LSPR appears in the visible region. The distribution of Ag nanoparticles obtained from HR-TEM images has been used to simulate absorption spectra and electric field distribution along Ag nanoparticles with the help of FDTD (Finite Difference Time Domain). Further, the ion irradiation results (experimental as well simulated) were compared with the annealed nanocomposite thin film and it was found that optical properties of heavily doped metal in the metal oxide matrix can be more improved by ion irradiation in comparison with thermal annealing.

Keywords: *nanocomposite; thin film; Ag-TiO_2; FDTD; ion irradiation*

1. Introduction

Nanocomposite materials of metal nanoparticles in dielectric matrix are an important subject of research due to their multifunctional properties in various fields such as solar cells [1, 2], photocatalysis [3–5], antibacterial activity [6, 7], and plasmonics [8–12]. The material of nanoparticles and the matrix in which nanoparticles are embedded directly plays a major role in localized surface plasmon resonance (LSPR). Besides, LSPR strongly depends on the shape and size of nanoparticles and interparticle separation [13–15]. Various dielectric materials have been used as a matrix for tuning LSPR position and also to maintain the separation between the nanoparticles.

Among metal oxides, titanium dioxide (TiO_2) has received great attention owing to its wide applications in solar cells [16, 17], antibacterial [18], photocatalytic [19, 20] and memristors [21, 22]. The inclusion of metal nanoparticles into TiO_2 matrix improves its properties which mainly depend on the crystallinity, stoichiometry of matrix, shape, size and filling fraction of nanoparticles. Swift Heavy Ion (SHI) irradiation helps to modify the properties of nanocomposites in a controlled way by selecting appropriate ion fluences and energies [23–26].

The aim of this paper is to study the effect of SHI irradiation on the plasmonic properties of Ag-TiO_2 nanocomposite thin films with a high concentration of Ag. The high filling fraction of metal nanoparticles in TiO_2 matrix is interesting because, at higher concentration, structural properties of the matrix remain unaffected by ion-irradiation. Due to SHI irradiation, the temperature of nanocomposite thin film does not increase up to the value which could modify the matrix properties. However, it is sufficient to induce modification in the properties of the metal nanoparticles. This may result

*E-mail: himanshumnit86@gmail.com

in the lower thermal conductivity of metal nanoparticles than that of matrix [27, 28]. Further, a comparative study of the properties of Ag-TiO_2 nanocomposite thin films modified by thermal annealing and SHI irradiation has been carried out. In addition to above, the experimental results were compared with simulated results and explained the position and existence of LSPR.

2. Experimental

Ag-TiO_2 nanocomposite thin films have been deposited on quartz, silicon and glass substrates by RF co-sputtering. Before deposition, the substrates were sequentially cleaned with acetone, methanol and trichloroethylene (TCE). TiO_2 powder (Alfa Aesar, ~99.9 %) was used to prepare the target. The size of the target holder and substrate holder was 5.08 and 12.7 cm, respectively. The substrate holder rotated to get uniform composition and thickness all over the substrates. Before the deposition, the vacuum was 1.6×10^{-4} Pa. For sputtering, argon gas medium was used at a pressure of 1 Pa and flow rate of 11 sccm. The thin films were deposited at a power of 75 W and room temperature. Ag-TiO_2 thin films were irradiated with 90 MeV Ni ion with fluences of 1×10^{12} ions/cm^2, 3×10^{12} ions/cm^2, 6×10^{12} ions/cm^2, 1×10^{13} ions/cm^2 in IUAC New Delhi. In case of 90 MeV Ni ions, the electronic (S_e) and nuclear (S_n) energy losses in the Ag-TiO_2 thin film were ~15.9 keV/nm and ~0.104 keV/nm, respectively, and the range of Ni ion was 10.3 μm which had been calculated from SRIM 2008 program. The energy loss curve of 90 MeV Ni in Ag (56 %)-TiO_2 is shown in Fig. 1.

As-deposited samples were sequentially annealed at 200 °C, 400 °C and 600 °C for 1 hour. The thickness of thin film and concentration of Ag were calculated by Rutherford backscattering (RBS) spectrometry (IUAC New Delhi). The angle between the detector and 2 MeV He^+ incident beam was 165°. X-ray diffraction (XRD) measurements were carried out using Panalytical X'Pert Pro X-ray diffractometer to determine the crystallinity of thin films. For optical properties measurement, irradiated and annealed nanocomposite

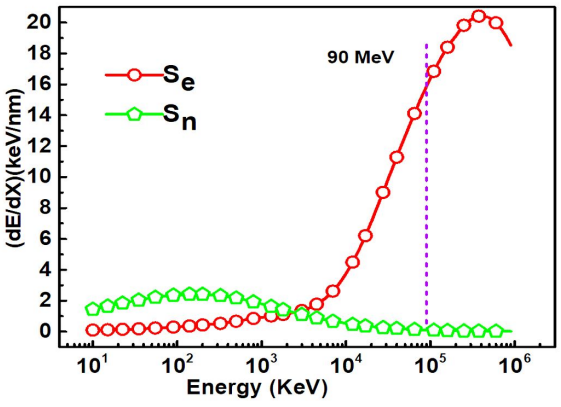

Fig. 1. Energy loss diagram for Ag (56 at.%)-TiO_2 nanocomposite thin film.

thin films were characterized by UV-Vis absorption spectroscopy using a dual beam Hitachi photospectrometer. Morphological studies of pristine and irradiated thin films have been done using HR-TEM (Tecnai G2 20 FEI S-Twin 200 kV). To simulate the absorption and electric field intensity, Lumerical FDTD software was used.

3. Results and discussion

3.1. SHI irradiation of Ag-TiO_2 thin film

3.1.1. Compositional, structural and morphological studies

For RBS analysis, Ag-TiO_2 thin films deposited on silicon have been used. The thickness of the nanocomposite thin film and concentration of Ag metal were determined by RUMP program and found to be ~50 nm and 56 at.%, respectively. A simulation obtained using RUMP program with depth profile, which confirmed the presence of Ti, Ag and O in nanocomposite thin film, is shown in Fig. 2. From the fitting view and depth profile, it is clear that Ag nanoparticles are distributed evenly along the depth of the thin film.

The XRD pattern of pristine and SHI irradiated Ag-TiO_2 nanocomposite thin films is presented in Fig. 3a. The peak position of Ag is observed at 38.1° and 44.3° which is in agreement with JCPDS Card No. 87-0720. For the fluence of 1×10^{12} ions/cm^2, Ag got amorphized and with

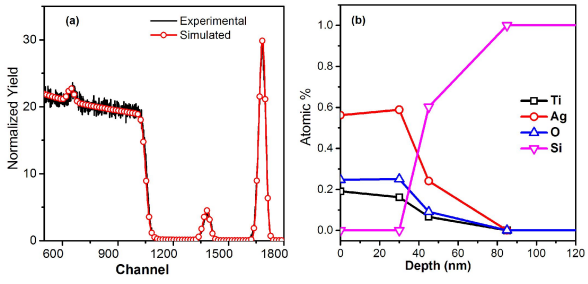

Fig. 2. (a) RBS of Ag (56 at.%)-TiO_2, simulation shown with red line + symbol and experimental data with black line; (b) depth profile of Ag (56 at.%)-TiO_2 nanocomposite thin film.

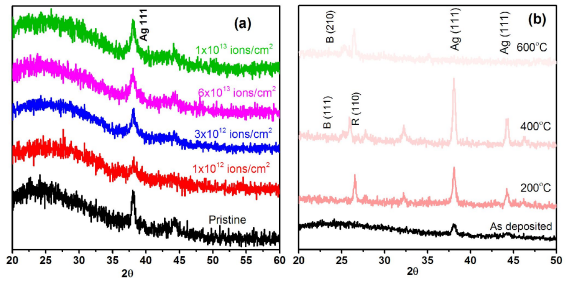

Fig. 3. (a) XRD of 90 MeV Ni ion thin film irradiated at different fluences; (b) XRD of thin film, sequentially annealed at 200 °C, 400 °C, 600 °C.

increasing the fluence from 3×10^{12} ions/cm^2 to 1×10^{13} ions/cm^2, crystallinity of Ag increased. On ion irradiation at low fluences, the Ag metal relaxed to the unstrained state and amorphous phase. With increasing the fluence of ion irradiation, the heat exchange between the ion and target material increases in the nanocomposite thin film. This heat exchange further promotes the recrystallization of Ag.

TEM images of pristine and SHI Ag-TiO_2 nanocomposite thin films irradiated with the fluence of 1×10^{13} ions/cm^2 are shown in Fig. 4. No diffraction peak corresponding to TiO_2 is observed in the as-deposited thin film which indicates amorphous nature of TiO_2. This is also evident from SAED pattern in Fig. 4e. When these thin films were irradiated by 90 MeV Ni ion with fluences of 1×10^{12} ions/cm^2, 3×10^{12} ions/cm^2, 6×10^{12} ions/cm^2, 1×10^{13} ions/cm^2, no change was observed in the phase of TiO_2; it remained in amorphous form. However, the crystallinity of Ag was affected by ion irradiation. After ion irradiation, the crystallinity of Ag was increased which is clearly seen in the SAED pattern (Fig. 4f).

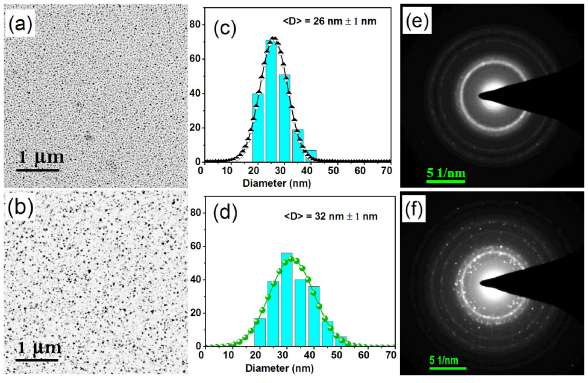

Fig. 4. (a), (b) plane view, bright field TEM images with (e), (f) SAED patterns and (c), (d) histograms of particle size distribution.

The topographical view of both as-deposited and ion irradiated at fluence 1×10^{16} ions/cm^2 samples is shown in Fig. 5a and Fig. 5b. Fig. 5c and Fig. 5d show the particle size distribution of pristine and ion irradiated thin films respectively. The average size of Ag nanoparticles for as-deposited and ion irradiated was calculated as ∼26 nm and ∼32 nm, respectively. To plot a histogram of particle size, ∼200 nanoparticles were considered. It is evident from the particle size distribution that after ion irradiation, the average particle size was increased by ∼6 nm. From Fig. 5 it has also been concluded that the interparticle separation between nanoparticles for the as-deposited sample is much lesser than their average particle size.

3.1.2. Absorption spectroscopy and FDTD simulation

Nanocomposite thin films deposited on glass were used to observe the effect SHI irradiation on optical properties and their UV-Vis absorption spectra are given in Fig. 6a. From Fig. 6a, it is clear that no LSPR has been observed in the visible range for the as-deposited thin film. The optical plasmonic behavior of metal nanoparticles embedded in a matrix depends on the morphology, interparticle separation, nanoparticles size

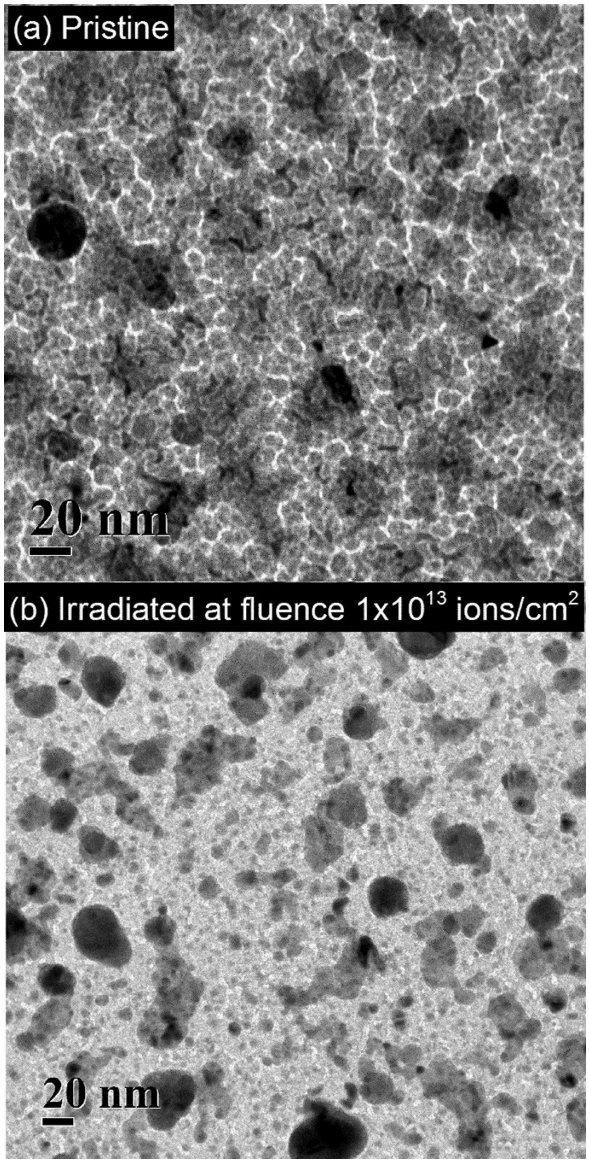

Fig. 5. Bright field images showing the effect of ion irradiation on interparticle separation.

distribution and dielectric constant of the matrix. Here, for Ag-TiO_2 (Ag 56 at.%) pristine thin film, the interparticle separation is minuscule compared to the nanoparticle size, which is clearly seen in Fig. 5a. The average nanoparticle size was calculated to be ∼26 nm. This minuscule interparticle separation results in LSPR lying in the infrared region and broadening of LSPR. When these thin films were irradiated by 90 MeV Ni ion, the absorption increased in the visible region. For the fluences of 1×10^{12} ions/cm^2 and 3×10^{12} ions/cm^2, there is an increment in absorbance in the region of 400 nm to 600 nm. At the fluence of 6×10^{12} ions/cm^2, the absorbance shifted towards the higher wavelength. However, at the fluence of 1×10^{13} ions/cm^2, broad LSPR is observed at the position of 566 nm.

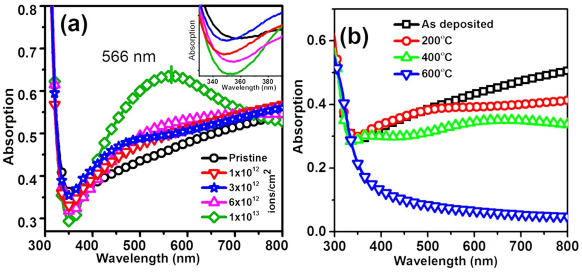

Fig. 6. (a) optical absorption spectra of nanocomposite thin film irradiated by 90 MeV Ni ion and (b) thin films sequentially annealed at 200 °C, 400 °C, 600 °C.

To study the plasmonic modification in Ag-TiO_2 nanocomposite thin films (pristine and 1×10^{13} ions /cm^2 irradiated) HR-TEM images (Fig. 5) were used for the simulation of absorption and electric field intensity distribution by FDTD method. Fig. 7a and Fig. 7b reveal the electric field distribution at the wavelength of 550 nm and Fig. 7c shows absorption obtained by FDTD simulation. In the simulation, we have used refractive index and extinction coefficient for TiO_2 from reference [29] and Ag (CRC) from FDTD software [30]. The monitor was placed at a distance of 10 nm from the top surface of the thin film. The vertical color bar represents the electric field intensity recorded on the monitor. The discrepancy from the experimental results from the fact that only a small part of the film was used for simulation. Before irradiation, the interparticle separation is very low, so the plasmonic coupling becomes more effective and it affects the LSPR of nearby nanoparticles, which results in increased absorption at a higher wavelength. This can be elucidated by using MAG (Maxwell-Garnet Theory) and Mie theory [31].

According to these theories, when nanoparticle size is increased, the higher order modes become more important and the nanoparticle polarizes non-homogenously. Therefore, due to these

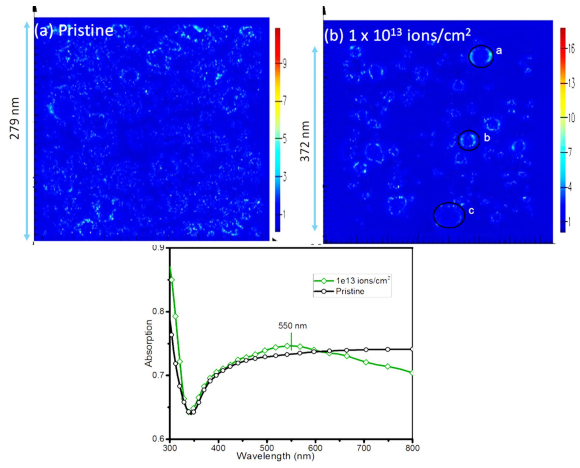

Fig. 7. Distribution of electric field intensity around Ag nanoparticles (a) simulation for pristine thin film (b) simulation for irradiated thin film at fluence 1×10^{13} ions/cm^2 at 550 nm (c) absorption spectra from simulation.

higher modes there is a shift in the plasmon position with increment in particle size and the plasmon bandwidth [32]. However, Mie theory is valid only for low concentration of nanoparticles in a solid matrix. In Mie theory, each nanoparticle is assumed to be separated by enough distance, and no LSPR effect on other nanoparticles is considered. In case of pristine thin film, Mie theory cannot be applied, as only a minuscule separation exists between the nanoparticles. This problem can be solved by MAG theory. This theory explains the plasmon resonance in nanoparticles having less interparticle separation. It considers the interparticle plasmonic effect on other nanoparticles and explains surface plasmon for densely packed nanoparticles in a host matrix. A combined model of these theories is given graphically in the Fig. 8. According to these theories, when the nanoparticle size is increased, its LSPR wavelength increases. If we consider two nanoparticles at low separation as given in Fig. 8, then, as the separation decreases, the interparticle plasmonic coupling becomes more effective and its LSPR wavelength increases. Those two particles play a role in LSPR and show complex absorption. These effects are observed in the FDTD simulation also. In Fig. 9a, the absorbed power is low at 350 nm and 750 nm compared to power absorbed at 550 nm. Absorption at 350 nm includes the LSPR due to small nanoparticles, which are seen in Fig. 9. When the wavelength is increased, the large nanoparticles effectively show absorption by LSPR. It can be seen in Fig. 7a, and Fig. 7b that the electric field intensity increases after irradiation and shows less interparticle plasmonic coupling effect compared to pristine thin film. The black circles (shown in Fig. 7b) are of the size of (a) 35 nm (b) 26 nm and (c) 50 nm. One can see that the particles (a) and (b) show good absorption at 550 nm, whereas the particle (c) which is larger than (a) and (b), partially absorbs power at 550 nm.

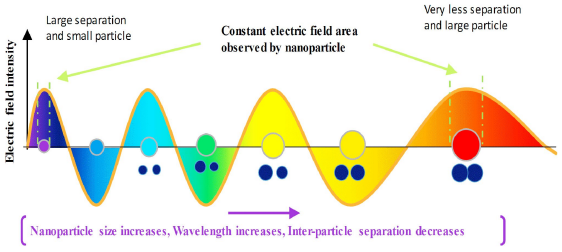

Fig. 8. Schematic diagram for the dependence of color/absorption on nanoparticle size and interparticle separation.

After SHI irradiation, the distribution of nanoparticles in the matrix and the optical properties of nanocomposite thin films have been modified. Earlier studies revealed the growth of metal nanoparticles in nanocomposite thin film under SHI irradiation [8]. After ion irradiation, growth in nanoparticles has been observed which is also confirmed by TEM and UV-Vis absorption results. The average particle size of the thin film irradiated with the highest fluence was calculated to be ~32 nm and shown in Fig. 4d. UV-Vis absorption graph (Fig. 6a) suggests that absorption increases for higher wavelength for pristine thin film. At low fluences 1×10^{12} ions/cm^2 and 3×10^{12} ions/cm^2, there is an increment in the LSPR intensity in the region of 400 nm to 500 nm. At the fluence 6×10^{12} ions/cm^2 the absorption in region of 400 nm to 500 nm shifted towards higher wavelength (500 nm to 600 nm) region. The most intense peak of LSPR has been observed after

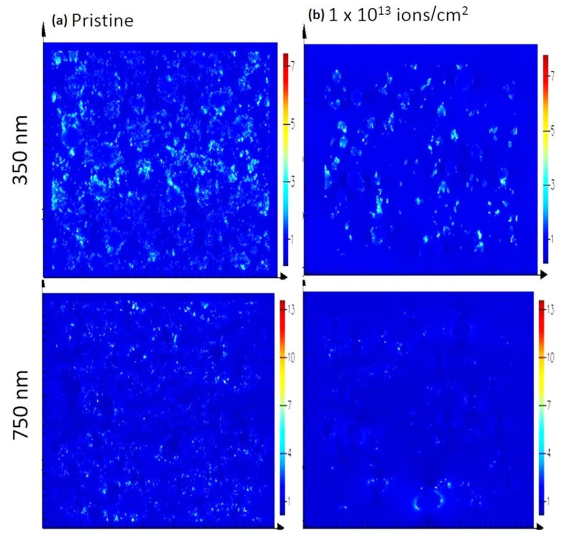

Fig. 9. Distribution of electric field intensity (a) simulation for pristine thin film at 350 nm and 750 nm (b) simulation for irradiated thin film at fluence 1×10^{13} ions/cm^2 at 350 nm and 750 nm.

irradiation at the fluence 1×10^{13} ions/cm^2 at 566 nm and its area was increased compared to other irradiated thin film, which reveals an increase in particle size and a number of particles. This result is in good agreement with the TEM results. As many clusters, atoms, and very small nanoparticles have combined to form new nanoparticles in the nanocomposite thin film, this led to enhancement in the LSPR absorption peak. The absorption in the region of 320 nm to 400 nm is due to the smaller nanoparticles, whose number decreases while increasing the ion fluences. This decrement is also in support of agglomeration of the smaller nanoparticles to form bigger ones due to the thermal energy provided by SHI ions. Simultaneously, the interparticle separation has been increased by ion irradiation, which resulted in lowering the interparticle coupling effect and broadening of LSPR, as well. As small nanoparticles and clusters are available in this region, the counts of absorption in the region of 320 nm to 400 nm are due to the smaller nanoparticles whose number decreases with increasing the ion fluences. The absorption peak remains broad because of the formation of Ag nanoparticles with irregular shapes, which leads to non-homogenous polarization.

3.2. Annealing of Ag-TiO_2 thin films

As discussed above, the plasmonic behavior changes with structural and morphological properties of filler and matrix. These structural and morphological properties can be modified by thermal annealing also. Fig. 6b shows UV-Vis absorption spectra of annealed nanocomposite thin films. Sequential annealing up to 400 °C has not caused any significant change in the plasmonic behavior of heavily doped Ag in the visible region. Low intensity peak has appeared at 500 nm and 650 nm for the annealing temperatures of 200 °C and 400 °C, respectively. Fig. 3 shows the XRD spectra of sequentially annealed nanocomposite thin films. The crystallinity of the TiO_2 host matrix varies insignificantly and in uncontrolled manner. The presence of mixed phase of rutile and brookite was observed after thermal annealing. Compared to the pristine thin films, annealed films showed higher crystallinity of matrix and also the agglomeration of Ag particles. The agglomeration increased with increasing annealing temperature, which caused the increase in the interparticle separation. As a result, the absorption of the thin films annealed at 200 °C and 400 °C was obtained in the visible region. After annealing at 600 °C, the absorption decreased significantly and no LSPR was observed. This reduction in absorption intensity is due to sublimation and plasmonic bleaching of Ag nanoparticles in the matrix. This sublimation of nanoparticles has also been supported by XRD and XPS studies (Fig. 10) of pristine and annealed thin films. After annealing at 600 °C, the diffraction peak in XRD disappeared and in XPS, the intensity of Ag 3d peak was found to be reduced compared to the pristine thin film.

Both annealed and ion irradiated nanocomposite thin films were systematically investigated. Comparatively, ion irradiation shows more flexibility in the modification of heavily doped Ag-TiO_2 nanocomposite thin films. The electronic energy transferred by SHI ions is converted into thermal energy and enhances the nucleation and growth of metallic nanoparticles. This thermal energy is very low as compared to the energy given during thermal annealing, but it is confined to low volume, so it is sufficient to modify the plasmonic

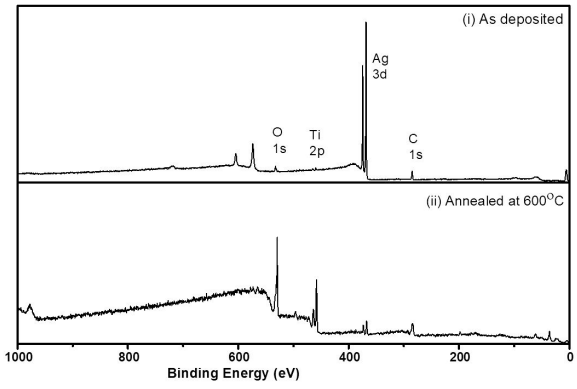

Fig. 10. XPS of pristine and 600 °C annealed thin film.

properties. By ion irradiation, the LSPR properties can be tuned easily rather than by annealing of Ag-TiO_2 nanocomposite thin film.

4. Conclusions

Heavily doped Ag-TiO_2 nanocomposite thin films were synthesized by RF co-sputtering. SHI irradiation caused remarkable changes in the morphological and plasmonic properties of the nanocomposite thin films. The average size of nanoparticles was increased and a minor red shift was observed with increasing the fluence. FDTD simulation was done for both pristine and irradiated thin film, which explains more clearly the existence of LSPR with the support from MAG theory. The growth of Ag nanoparticles and occurrence of redshift was discussed in detail and attributed to agglomeration due to massive electronic energy transferred by swift heavy ion irradiation. It can be concluded that for a higher concentration of Ag in TiO_2, the SHI irradiation is more effective in modification of plasmonic properties of the nanocomposite thin films than the thermal annealing. The enhancement in LSPR in visible region by SHI irradiation is advantageous for photocatalytic activities and biomaterials.

Acknowledgements

This work is supported under the Project (UFR-54302) by the IUAC New Delhi.

References

[1] MUDULI S., GAME O., DHAS V., VIJAYAMOHANAN K., BOGLE K.A., VALANOOR N., OGALE S.B., *Sol. Energy,* 86, (2012), 1428.

[2] ZHANG X., LIU J., LI S., TAN X., YU M., DU J., *RSC Adv.,* 3, (2013), 18587.

[3] KUMAR A., PATEL A.S., MOHANTY T., *J. Phys. Chem. C,* 116, (2012), 20404.

[4] WODKA D., BIELAŃSKA E., SOCHA R.P., ELŻBIECIAK WODKA M., GURGUL J., NOWAK P., WARSZYŃSKI P., KUMAKIRI I., *ACS Appl. Mater. Interfaces,* 2, (2010), 1945.

[5] CHEN D., CHEN Q., GE L., YIN L., FAN B., WANG H., LU H., XU H., ZHANG R., SHAO G., *Appl. Surf. Sci.,* 284, (2013), 921.

[6] YU B., LEUNG K.M., GUO Q., LAU W.M., YANG J., *Nanotechnology,* 22, (2011), 115603.

[7] AKHAVAN O., *J. Colloid Interface Sci.,* 336, (2009), 117.

[8] MISHRA Y.K., AVASTHI D.K., KULRIYA P.K., SINGH F., KABIRAJ D., TRIPATHI A., PIVIN J.C., BAYER I.S., BISWAS A., *Appl. Phys. Lett.,* 90, (2007), 073110.

[9] KUMAR M., SANDEEP C.S.S., KUMAR G., MISHRA Y.K., PHILIP R., REDDY G.B., *Plasmonics,* 9, (2014), 129.

[10] MOHAPATRA S., MISHRA Y.K., WARRIER A.M., PHILIP R., SAHOO S., ARORA A.K., AVASTHI D.K., *Plasmonics,* 7, (2012), 25.

[11] AVASTHI D.K., MISHRA Y.K., SINGHAL R., KABIRAJ D., MOHAPATRA S., MOHANTA B., GOHIL N.K., SINGH N., *J. Nanosci. Nanotechnol.,* 10, (2010), 2705.

[12] SINGHAL R., KABIRAJ D., KULRIYA P.K., PIVIN J.C., CHANDRA R., AVASTHI D.K., *Plasmonics,* 8, (2013), 295.

[13] NOGUEZ C., *J. Phys. Chem. C,* 111, (2007), 3806.

[14] GHOSH S.K., PAL T., *Chem. Rev.,* 107, (2007), 4797.

[15] KELLY K.L., CORONADO E., ZHAO L.L., SCHATZ G.C., *J. Phys. Chem. B,* 107, (2003), 668.

[16] SUNG Y.M., *Energy Procedia,* 34, (2013), 582.

[17] RICHARDS B.S., *Sol. Energy Mater. Sol. Cells,* 79, (2003), 369.

[18] WEI-GUO X., AN-MIN C., QIANG Z., *J. Wuhan Univ. Technol. Sci. Ed.,* 19, (2004), 16.

[19] CHEN F., CAO F., LI H., BIAN Z., *Langmuir,* 31, (2015), 3494.

[20] ŠEGOTA S., ĆURKOVIĆ L., LJUBAS D., SVETLIČIĆ V., HOURA I.F., TOMAŠIĆ N., *Ceram. Int.,* 37, (2011), 1153.

[21] DURAISAMY N., MUHAMMAD N.M., KIM H.C., JO J.D., CHOI K.H., *Thin Solid Films,* 520, (2012), 5070.

[22] BOUSOULAS P., MICHELAKAKI I., TSOUKALAS D., *J. Appl. Phys.,* 115, (2014), 034516.

[23] SINGHAL R., AGARWAL D.C., MISHRA Y.K., SINGH F., PIVIN J.C., CHANDRA R., AVASTHI D.K., *J. Phys. D. Appl. Phys.,* 42, (2009), 155103.

[24] AVASTHI D. K., MEHTA G. K., *Swift Heavy Ions for Materials Engineering and Nanostructuring,* Springer, Netherlands: Dordrecht, 2011.
[25] GUPTA A., SINGHAL R., NARAYAN J., AVASTHI D.K., *J. Mater. Res.,* 26, (2011), 2901.
[26] SINGHAL R., PIVIN J.C., CHANDRA R., AVASTHI D.K., *Surf. Coatings Technol.,* 229, (2013), 50.
[27] KIM D.J., KIM D.S., CHO S., KIM S.W., LEE S.H., KIM J.C., *Int. J. Thermophys.,* 25, (2004), 281.
[28] ZHANG Y., SCHWARTZBERG A. M., XU K., GU C., ZHANG J. Z., BURDA C., ELLINGSON R.J., *Physical Chemistry of Interfaces and Nanomaterials IV,* 5929, (2005), 592912.
[29] DAVIS K.O., JIANG K., HABERMANN D., SCHOENFELD W. V., *IEEE J. Photovoltaics,* 5, (2015), 1265.
[30] `http://www.lumerical.com/tcad-products/fdtd/`.
[31] HAGEMANN H.J., GUDAT W., KUNZ C., *J. Opt. Soc. Am.,* 65, (1975), 742.
[32] LINK S.S., EL-SAYED M.A., *Int. Rev. Phys. Chem.,* 19, (2000), 409.

Received 2017-11-17
Accepted 2018-10-03